Supporting Information

One-dimensional nanotube of metal-organic framework boosts charge separation and photocatalytic hydrogen evolution from water: synthesis and underlying understanding

Lifang Liu†[a,b], Yejun Xiao†[c], Xiangyang Guo[a], Wenjun Fan[a], Nengcong Yang[a,b], Chunmei Jia[a], Shengye Jin[c], and Fuxiang Zhang*[a]

[a] State Key Laboratory of Catalysis, Dalian Institute of Chemical Physics, Chinese Academy of Sciences, Dalian National Laboratory for Clean Energy, Dalian 116023, China

[b] Center of Materials Science and Optoelectronics Engineering, University of Chinese Academy of Sciences, Beijing 100049, China

[c] State Key Laboratory of Molecular Reaction Dynamics and Dynamics Research Center for Energy and Environmental Materials, Dalian Institute of Chemical Physics, Chinese Academy of Sciences, Dalian 116023, China

†These authors contributed equally: Lifang Liu, Yejun Xiao

E-mail: fxzhang@dicp.ac.cn

Methods

Materials

1,3,6,8-tetrakis (p-benzoic acid) pyrene (H$_4$TBAPy) was purchased from Jilin Chinese Academy of Sciences-Yanshen technology Co. Ltd, MnCl$_2$·4H$_2$O, N, N-dimethylformamide (DMF), Dioxane, and Methanol (MeOH) were bought by Sinopharm Chemical Reagent Shenyang Co.Ltd. All chemicals were used without further purification.

Synthesis of Mn-TBAPy-NT and Mn-TBAPy-SC

MnCl$_2$·4H$_2$O (2.3 mg) and H$_4$TBAPy (5 mg) were dissolved in DMF solvent (4 mL). The MnCl$_2$·4H$_2$O solvent was dropped into H$_4$TBAPy solution under stirring 30 min and then transferred into a 25 mL Teflon-lined stainless-steel autoclave. The autoclave was heated at 120 ^{o}C for 6 h and then cooled to room temperature. Yellow powder of Mn-TBAPy-NT nanotubes were obtained by washing with DMF, mixed solution of MeOH and H$_2$O three times and freeze drying.

According to previous synthesis methods of Mn-TBAPy-SC[1], MnCl$_2$·4H$_2$O (29.7 mg) and H$_4$TBAPy (66.6 mg) were dispersed in a mixed solution of DMF, H$_2$O, and Dioxane (4 mL, 2:1:1, v/v/v), and sealed in a 25 mL Teflon-lined stainless-steel autoclave. The autoclave was heated at 120 ^{o}C for 72 h, and then cooled to room temperature at a rate of 5 ^{o}C h^{-1}. Yellow powder of Mn-TBAPy-SC single crystal were obtained by washing with DMF and CH$_3$CN four times, and dried in a vacuum oven overnight.

Preparation of Pt/Mn-TBAPy-NT and Pt/Mn-TBAPy-SC

H$_2$PtCl$_6$ aqueous solution (60 µL, 1 mg mL^{-1}) was added into 20 mg Mn-TBAPy-NT or Mn-TBAPy-SC powder, and then dried at 80 ^{o}C under stirring. The platinum-modified Mn-TBAPy-NT or Mn-TBAPy-SC (Pt/Mn-TBAPy-NT and Pt/Mn-TBAPy-SC, 0.3 wt% Pt) were reduced with 5% H$_2$/Ar at 473 K for 2 h.

Characterization

XRD: XRD measurements were tested by SmartLab X-ray diffractometer (Cu Kα radiation, λ = 1.5418 Å). A scan rate of 5 ^{o} min^{-1} was applied in the range of 5-40°.

UV-vis: UV-vis diffuse reflectance spectra (DRS) were recorded on a UV-vis spectrophotometer (SHIMADZU UV-2600) at room temperature equipped with an integrating sphere using standard BaSO$_4$ white powder as reference for the baseline correction.

BET: The Brunauer-Emmett-Teller (BET) surface area experiment was performed on Micromeritics ASAP 2000 adsorption analyzer at 77 K.

FT-IR: Fourier transform infrared (FT-IR) spectra were measured by thermofisher scientific-Nicolet iS50 system from KBr pellets.

XPS: The binding energies were measured by X-ray photoelectron spectroscopy (XPS) and using Thermo Fisher ESCALAB250xi with a monochromatic Al Ka X-ray source.

SEM: Scanning electron microscope (SEM) images were measured by Quanta 200F and JSM-7900F.

TEM: Transmission electron microscope (TEM) images were measured by JEM-2100 microscope.

EPR*: The synthesized Mn-TBAPy-SC and Mn-TBAPy-NT powder samples was transferred into the EPR reactor and the EPR spectra were obtained by using Bruker A200 at 110K.

Raman spectra：Raman spectra were collected using 785 nm diode-pumped solid-state laser (Changchun New Industries Optoelectronics Technology Co., Ltd.) and a commercial Raman spectrometer (Invia, Renishaw plc.).

Time-resolved fluorescence decay kinetics: Samples are measured by a home-built PL-scanned imaging microscope coupled with time-correlated single photon counting (TCSPC) module. Excitation of the sample is achieved with a pulsed 375 nm laser (PDL 800-B, PicoQuANT).

Femtosecond transient absorption spectroscopy (TA) measurement

The femtosecond transient absorption (fs-TA) setup was used to record the TA date. which is based on a regenerative amplified Ti:sapphire laser system from Coherent (800 nm, 35 fs, 6 mJ/pulse, and 1 kHz repetition rate), nonlinear frequency mixing techniques and the Femto-TA100 spectrometer (Time-Tech Spectra). Briefly, the 800 nm output pulse from the regenerative amplifier was split in two parts with a 50% beam splitter. The transmitted part was used to pump a TOPAS Optical Parametric Amplifier (OPA) which generates a wavelength-tunable laser pulse from 250 nm to 2.5 m as pump beam. The reflected 800 nm beam was split again into two parts. One part with less than 10% was attenuated with a neutral density filter and focused into a 2 mm thick sapphire window to generate a white light continuum (WLC) from 420 nm to 800 nm used for probe beam. The probe beam was focused with an Al parabolic reflector onto the sample. After the sample, the probe beam was collimated and then focused into a fiber-coupled spectrometer with CMOS sensors and detected at a frequency of 1 kHz. The intensity of the pump pulse used in the experiment was controlled by a variable neutral-density filter wheel. The delay between the pump and probe pulses was controlled by a motorized delay stage. The pump pulses were chopped by a synchronized chopper at 500 Hz

and the absorbance change was calculated with two adjacent probe pulses (pump-blocked and pump-unblocked). All experiments were performed at room temperature.

Nanosecond transient absorption measurement

Nanosecond TA experiments were measured with the EOS spectrometer (Nano-TA100, Time-Tech Spectra). The pump beam is generated in the same way as the femtosecond TA experiment described above. A different white light continuum (380–1700 nm, 0.5 ns pulse width, 20 kHz repetition rate) was used, which was generated by focusing a Nd:YAG laser into a photonic crystal fiber. The delay time between the pump and probe beam was controlled by a digital delay generator 4 (CNT-90, Pendulum Instruments).

XAFS data analysis

The X-ray absorption fine structure spectra at the Mn k-edge was collected at the 1W1B beamline of Beijing Synchrotron Radiation Facility (BSRF). The datas were collected in fluorescence mode using a Lytle detector and the corresponding reference samples were collected in transmission mode.

The acquired EXAFS data were processed according to the standard procedures using the ATHENA module of Demeter software packages. The EXAFS spectra were obtained by subtracting the post-edge background from the overall absorption and then normalized by the edge-jump step. Subsequently, the $\chi(k)$ data of the EXAFS spectra were Fourier transformed to real $(R)^4$ space using a handing window (dk=1.0 Å^{-1}) to separate the EXAFS contributions from different coordination shells. To obtain the quantitative structural parameters around central atoms, least-squares curve parameter fitting was performed using the ARTEMIS module of Demeter software packages. The following EXAFS equation was used:

$$\chi(k) = \sum(N_j S_0^2 F_j(k)/kRj^2)\bullet\exp[-2k^2\sigma_j^2]\bullet\exp[-2R_j/\lambda(k)]\bullet\sin[2kR_j+\phi_j(k)].$$

The theoretical scattering amplitudes, phase shifts, and the photoelectron mean free path of all paths were calculated. S_0^2 is the amplitude reduction factor, $F_j(k)$ is the effective curved-wave backscattering amplitude, N_j is the number of neighbors in the jth atomic shell, R_j is the distance between the X-ray absorbing central atom and the atoms in the jth atomic shell (backscattered), λ is the mean free path in Å, $\phi_j(k)$ is the phase shift (including the phase shift for each shell and the total central atom phase shift), σ_j is the Debye-Waller parameter of the jth atomic shell (variation of distances around the average R_j). The functions $F_j(k)$, λ and $\phi j(k)$ were calculated with the ab initio code FEFF9. The additional details for EXAFS simulations are given below. All fits were performed in the R space with k-weight of 2, while phase correction was also applied in the first coordination shell to make R value close to the physical interatomic distance between the absorber and shell scattered. The coordination numbers of model samples were

fixed as the nominal values. The obtained S_0^2 was fixed in the subsequent fitting, while the internal atomic distances R, Debye-Waller factor σ^2, and the edge-energy shift Δ were allowed to run freely.

Preparation of work electrode and photoelectrode

The synthesized catalyst (5 mg) was dispersed into 0.05 % Nafion MeOH solution (0.1 mL) under ultrasonically treating for 30 min, and then the 10 μL suspension was dropped onto the surface of the cleaned FTO substrate.

Photocatalytic Reactions for Hydrogen Evolution

Photocatalyst (20 mg) was added into a Pyrex top-irradiation type reaction vessel which connected to an evacuation system containing a mixture of 15 mM ascorbic acid (hole sacrificial agent), deionized water (10 mL), and MeOH (90 mL) for Pt/Mn-TBAPy-NT and Pt/Mn-TBAPy-SC. After that, the reaction solution was degassed completely by a vacuum pump for 15 min under stirring. Finally, the sample was irradiated by a 300 W xenon lamp equipped with a 420 nm optical filter, and the cooling water was used to keep the reaction suspension at 15 °C by circular cooling water device. The gas products were analyzed by gas chromatography (Shimadzu, GC-2014, TCD, Ar carrier). It should be pointed out that during the reaction conditions the Mn-TBAPy-SC sample will be continuously exfoliated and transferred into nanotubes, so its photocatalytic activity evaluation was carried out for 15 mins to reduce the influence of formed nanotubes on the activity as possible as we can.

**Measurement of apparent quantum efficiency (AQE)**

Photocatalyst Pt/Mn-TBAPy-NT (20 mg) was added into a Pyrex top-irradiation type reaction vessel containing a mixture of 15 mM ascorbic acid (hole sacrificial agent), deionized water (10 mL), and MeOH (90 mL), which connected to an evacuation system. The light source is 300 W Xe lamp with a 420 nm, 440 nm, 460 nm, 480 nm, 520 nm band-pass filter. The number of incident photons reaching the solution was measured by using a calibrated Si photodiode (LS-100, EKO Instruments Co., LTD.). The AQE (ϕ) was calculated as following equation[2]:

$$AQE = \frac{AR}{I} \times 100 \quad (1)$$

Where, A represents a coefficient (2 for H_2 evolution), R represents the evolution rate of H_2, *I* represents the number of photons reaching the reaction solution. The total numbers of incident photons at the wavelength of 420 nm, 440 nm, 460 nm, 480 nm, 520 nm were measured to be 1.50×10^{20} photons h^{-1}, 2.09×10^{20} photons h^{-1}, 2.78×10^{20} photons h^{-1}, 3.07×10^{20} photons h^{-1}, 2.84×10^{20} photons h^{-1}, respectively. The H_2 evolution rates under the wavelengths of 420 nm,

440 nm, 460 nm, 480 nm, 520 nm were tested to be 14.59 µmol h^{-1}, 20.93 µmol h^{-1}, 25.39 µmol h^{-1}, 25.66 µmol h^{-1}, and 1.36 µmol h^{-1} respectively.
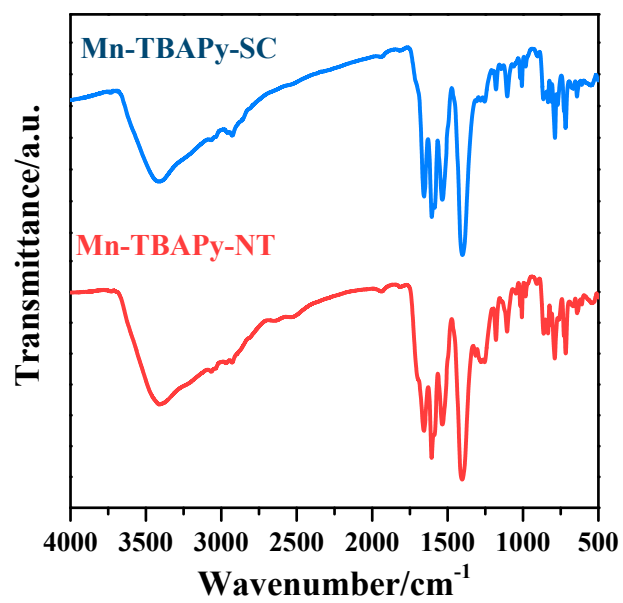
Supplementary Figures
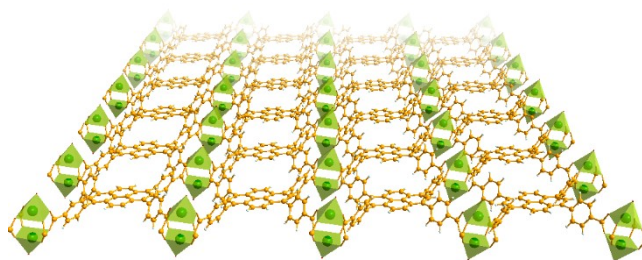
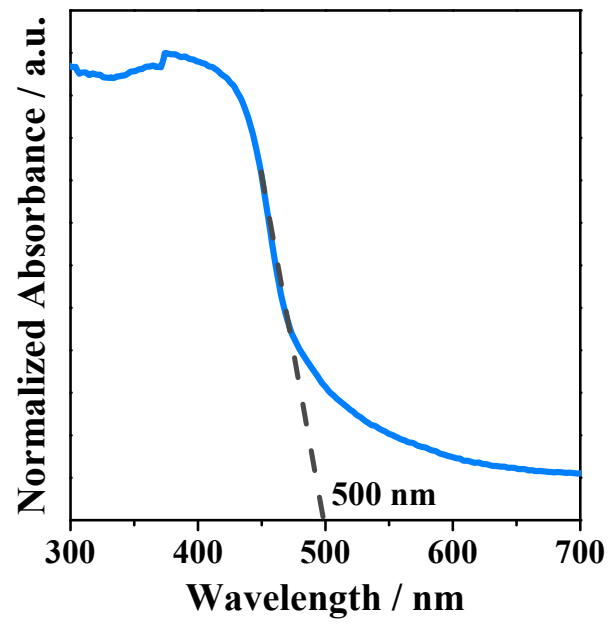**Fig. S1** 2 D layer structure of Mn-TBAPy.
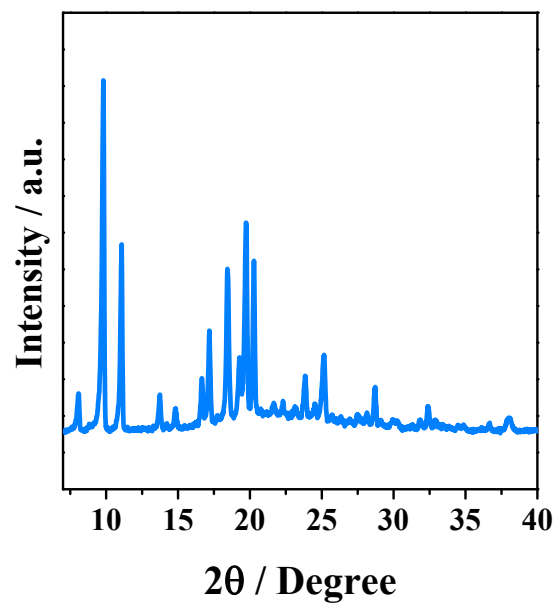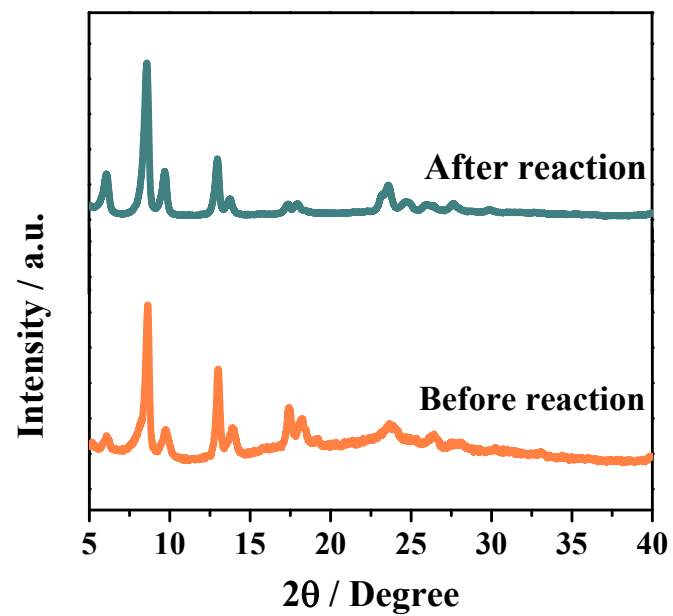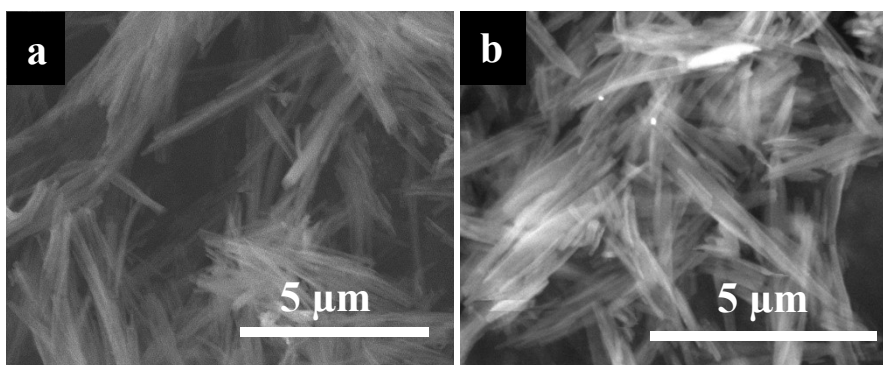
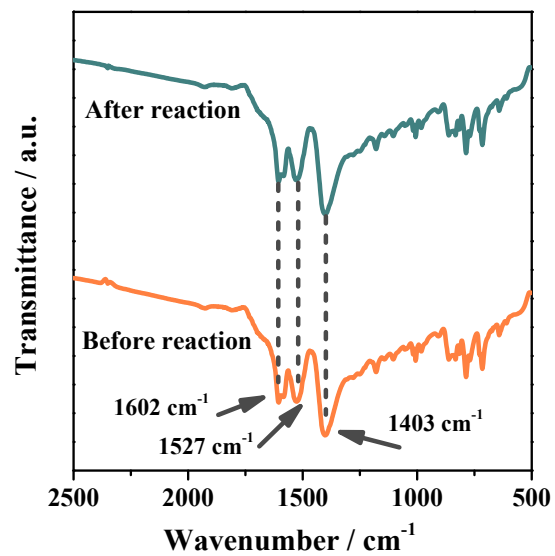**Fig. S2** XRD patterns of Mn-TBAPy-SC.

Fig. S3 FT-IR spectra of Mn-TBAPy-SC and Mn-TBAPy-NT nanotubes.

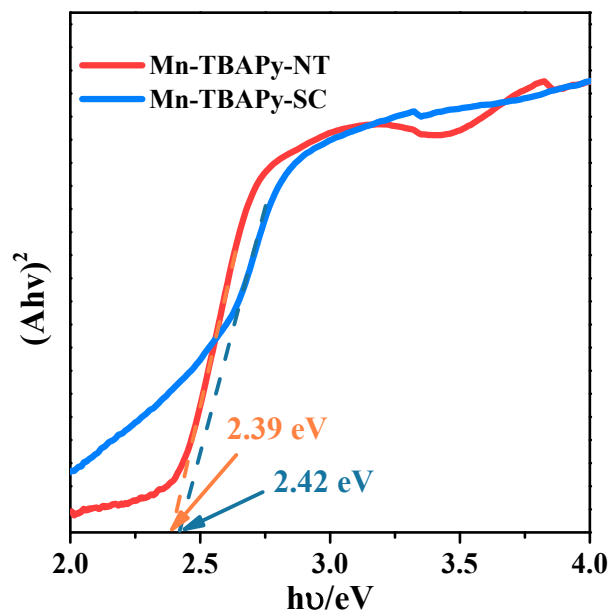**Fig. S4** UV-vis diffuse reflectance spectrum of Mn-TBAPy-SC.

Fig. S5 XRD patterns of Pt/Mn-TBAPy-NT nanotubes before and after 12 h H_2 evolution reaction.
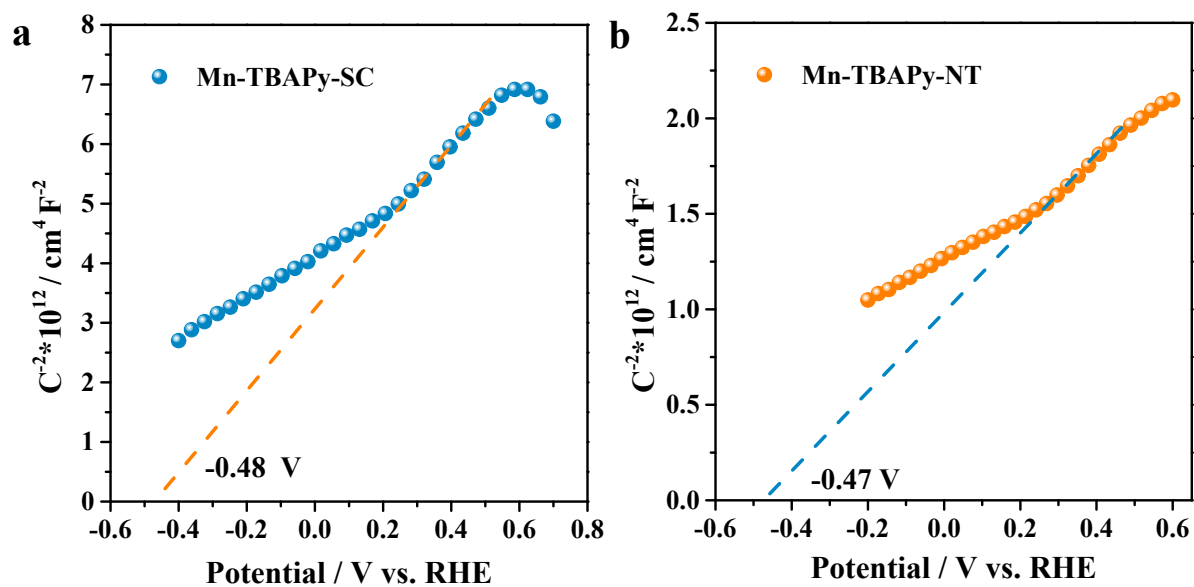
**Fig. S6** SEM images of Pt/Mn-TBAPy-NT nanotubes before a) and after b) 12 h H_2 evolution reaction.

Fig. S7 FT-IR spectra of Pt/Mn-TBAPy-NT nanotubes before and after 12 h H_2 evolution reaction.

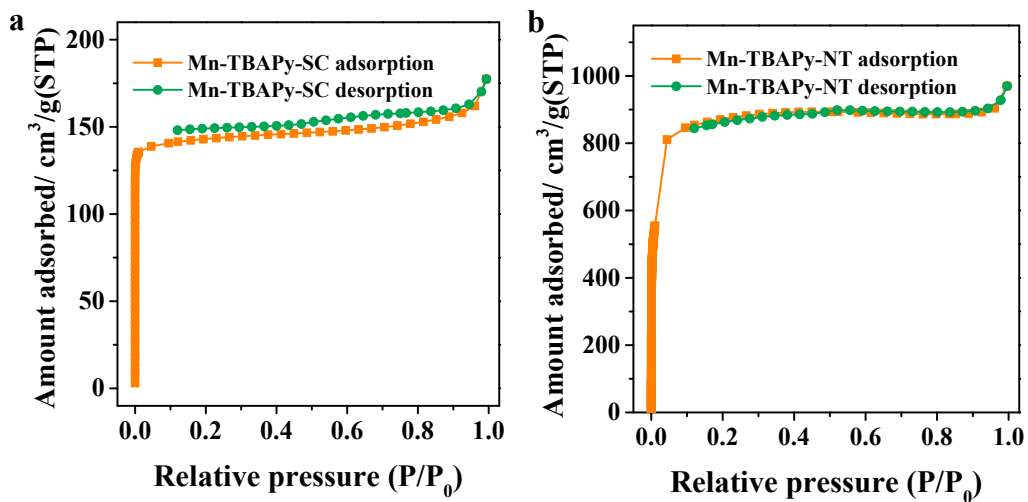**Fig. S8** Tauc plots of Mn-TBAPy-NT nanotubes and Mn-TBAPy-SC single crystal samples.

Fig. S9 Mott-Schottky plots of a) Mn-TBAPy-SC single crystal and b) Mn-TBAPy-NT nanotubes. The samples were droped on the FTO electrode and measurement frequency is 1 kHz.
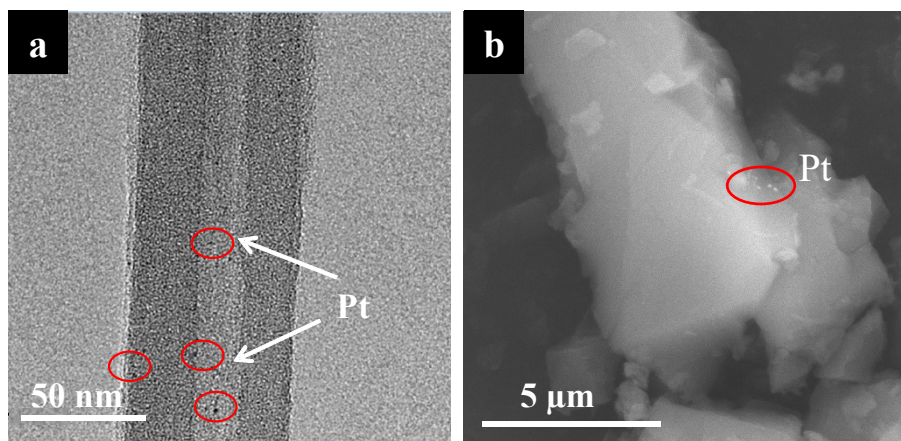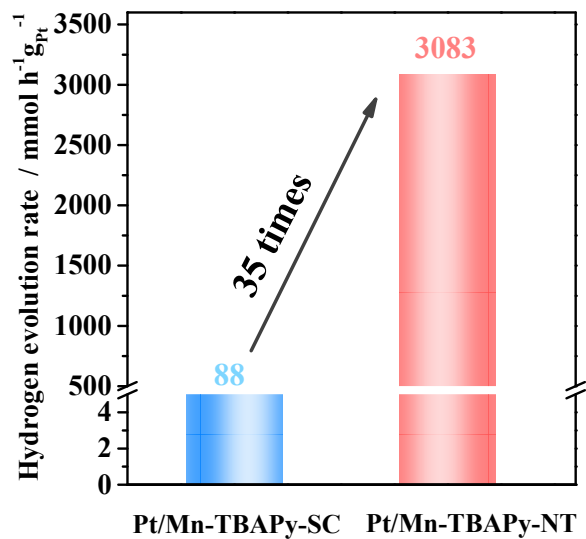
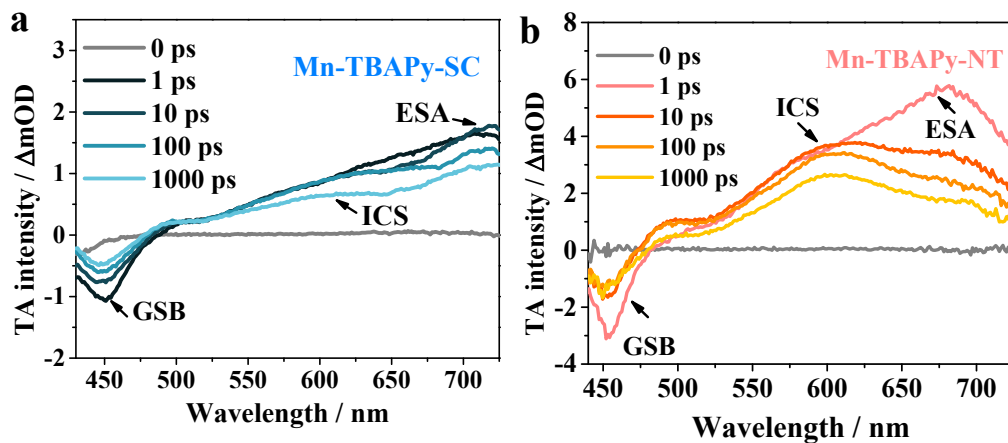**Fig. S10** a) TEM image of Pt/Mn-TBAPy-NT and b) SEM image of Pt/Mn-TBAPy-SC.

Fig. S11 N$_2$-adsorption/desorption isotherms (77 K) of a) Mn-TBAPy-SC and b) Mn-TBAPy-NT. The BET surface areas of Mn-TBAPy-SC and Mn-TBAPy-NT are 416 m^2 g^{-1} and 3243 m^2 g^{-1}, respectively.

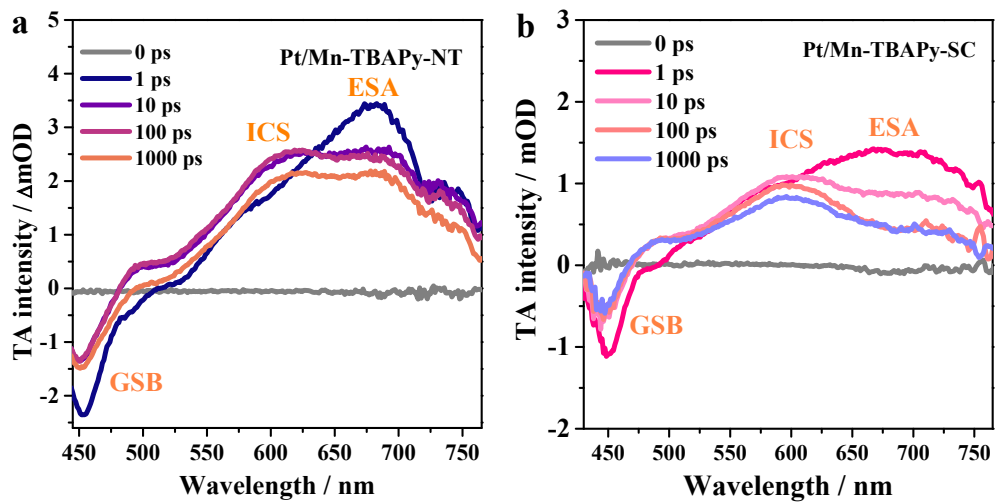**Fig. S12** Photocatalytic H_2 evolution rates of Mn-TBAPy-NT and Mn-TBAPy-SC after normalized to Pt content.

Fig. S13 Femtosecond transient absorption (fs-TA) spectra of a) Mn-TBAPy-SC and b) Mn-TBAPy-NT.
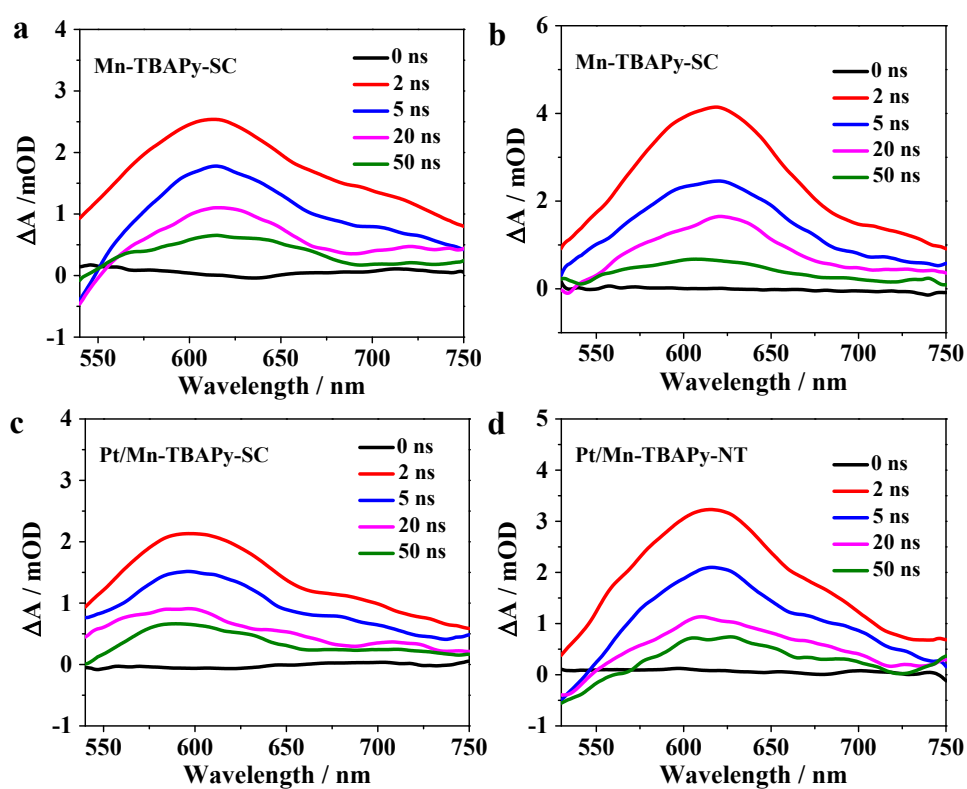
Fig. S14 Nanosecond transient absorption (ns-TA) spectra of a) Mn-TBAPy-NT, b) Mn-TBAPy-SC, c) Pt/Mn-TBAPy-NT, and d) Pt/Mn-TBAPy-SC at indicated delay times under excitation at 400 nm.

Fig. S15 Femtosecond transient absorption (fs-TA) spectra of a) Pt/Mn-TBAPy-NT and b) Pt/Mn-TBAPy-SC at indicated delay times under excitation at 400 nm.
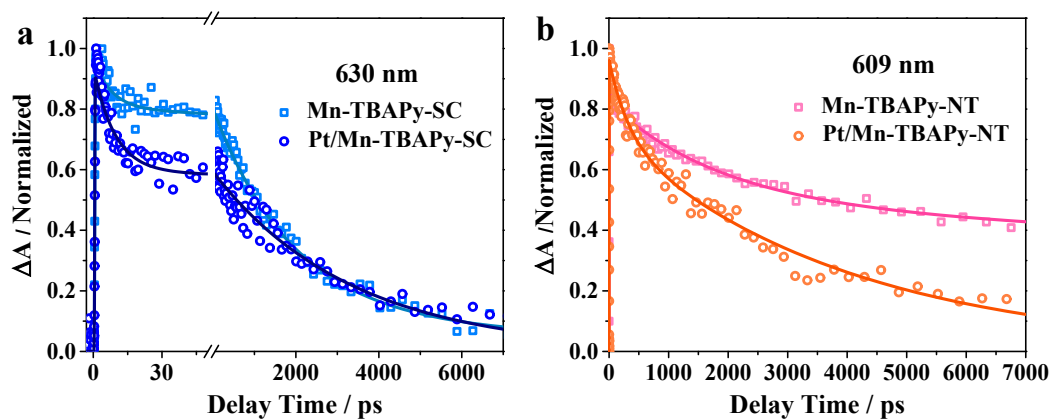
Fig. S16 Comparison of normalized femtosecond transient absorption (fs-TA) kinetics probed at indicated wavelengths 400 nm of a) Mn-TBAPy-SC and Pt/Mn-TBAPy-SC, b) Mn-TBAPy-NT and Pt/Mn-TBAPy-NT.
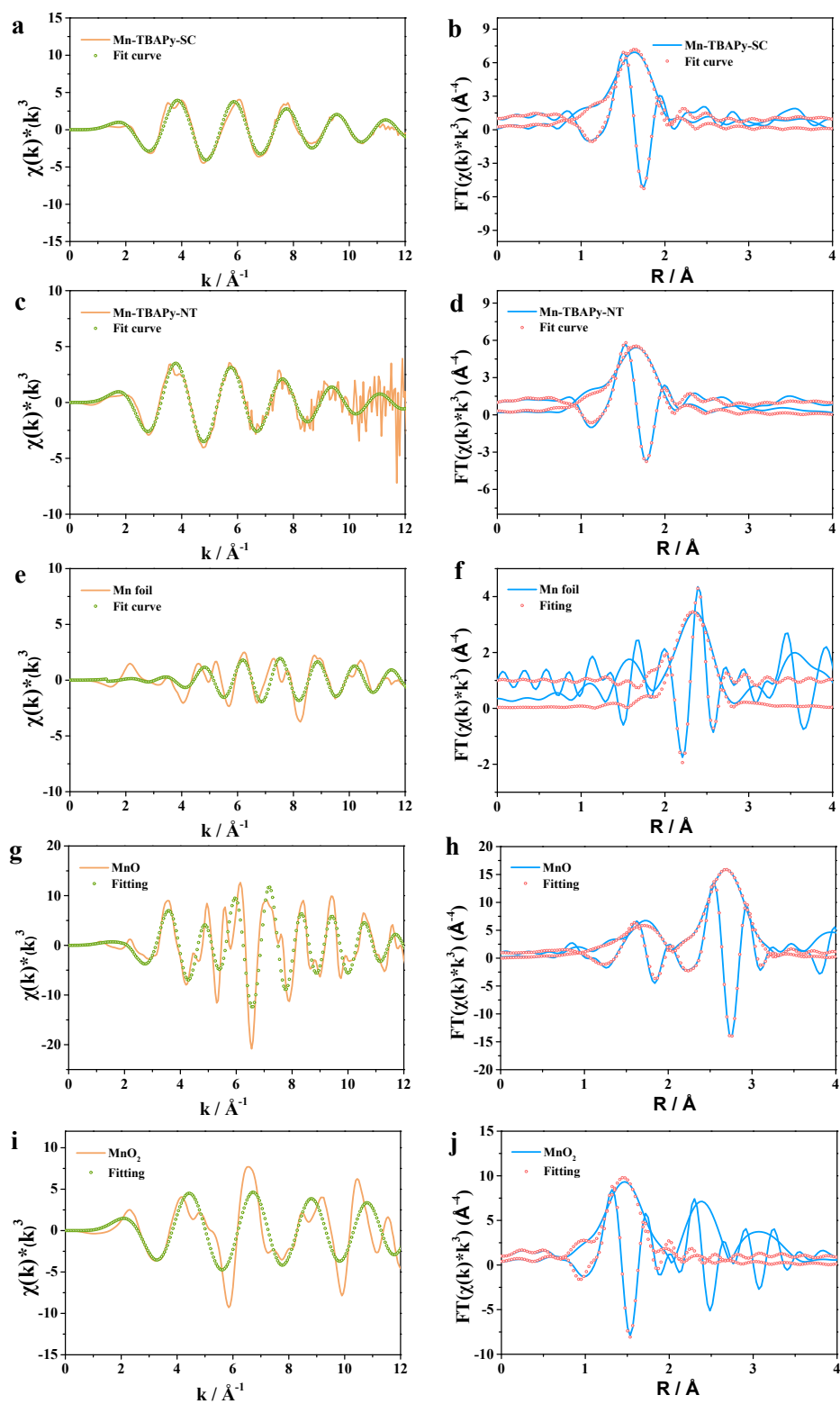
Fig. S17 Mn K-edge, Mn R space EXAFS, and the curve fitting for Mn-TBAPy-SC, Mn-TBAPy-NT, Mn-foil, MnO, and MnO$_2$ reference samples.
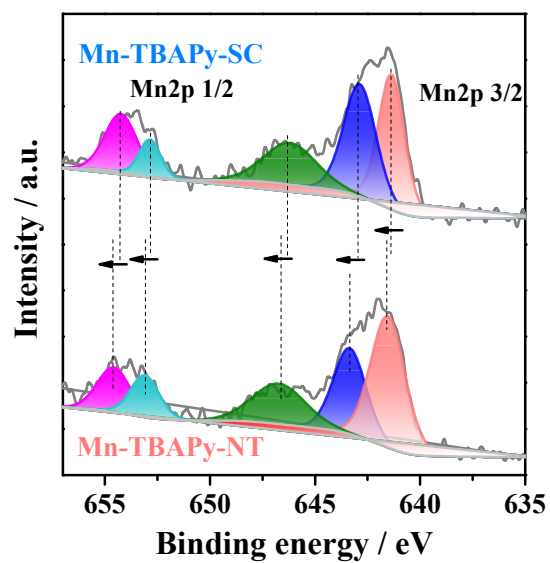
Fig. S18 X-ray photoelectron spectra (XPS) of Mn-TBAPy-SC and Mn-TBAPy-NT.
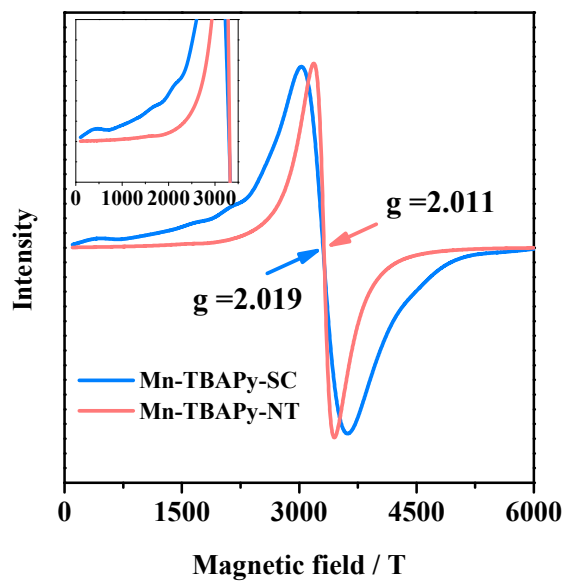
Fig. S19 Comparison of the EPR spectra of Mn-TBAPy-SC and Mn-TBAPy-NT measured at 77 K. The hyperfine structure for Mn ion disappears in Mn-TBAPy-NT, and the g value changes from 2.011 to 2.019 on both samples, indicating the change of local chemical environment of Mn ion.

Supplementary Tables

Table S1 Comparison of photocatalytic water splitting activities and AQEs value for typical MOFs photocatalysts.

Photocatalysts	Band gap [eV]	H_2 evolution	AQE %	Dimension	Light source	References
Pt/Mn-TBAPy-NT	2.42	203.5 μmol·h^{-1}	11.7 420 nm	1D	300 W Xe lamp λ≥420 nm	**This work**
Pt/20%-MIL-125-(SCH$_3$)$_2$	1.52	58.4 μmol·h^{-1}	8.9 420 nm	-	300 W Xe lamp λ≥420 nm	Angew. Chem. Int. Ed. 2018, 57, 9864-9869.
Pt/MIL(Ti)-80%	2.6	53 μmol·h^{-1}	4.0 420 nm	2D	300 W Xe lamp λ≥420 nm	Appl. Catal. B 2023, 338, 123094
Pt/Mn-TBAPy-NS	2.42	1.50 μmol h^{-1}	-	2D	300 W Xe lamp	Sci. China. Chem. 2020, 63, 1765 −1760
Ni$_1$-S/MOF	2.8	6.8 μmol h^{-1}	-	3D	300 W Xe lamp λ≥380 nm	J. Am. Chem. Soc. 2021, 143, 12220−12229
MUV-10(Ca)/Pt	3.1	6.77 μmol h^{-1}	-	3D	300 W Xe lamp UV-visible	Angew. Chem. Int. Ed. 2018, 130, 8589 −8593
ACM-1/Pt	2.3	67 μmol h^{-1}	0.15 440 nm	3D	300 W Xe lamp λ≥380 nm	Angew. Chem. Int. Ed. 2020, 59, 13468 −13472
NH$_2$-MIL-101/Pt	-	4.8 μmol h^{-1}	-	3D	500 W Xe/Hg lamp λ≥420 nm	Chem. Commun. 2014, 50, 11645-11648
NH$_2$-MIL-125(Ti)/Pt	2.6	3.67 umol h^{-1}	-	3D	300 W Xe lamp λ≥420 nm	J. Phys. Chem. C. 2012, 116, 20848−20853
Al-PMOF/Pt	-	0.8 μmol h^{-1}	-	3D	300 W Xe lamp λ≥420 nm	Angew. Chem. Int. Ed. 2012, 51, 7440 −7444
Pt$_{NP}$/SnO$_2$/UiO-66-NH$_2$	2.6	42.3 μmol h^{-1}	-	3D	300 W Xe lamp λ≥420 nm	Adv. Mater. 2022, 34, 2109203
MoO$_3$/MIL-125-NH$_2$	2.6	20 μmol h^{-1}	0.41 380 nm	3D	300 W Xe lamp λ≥380 nm	Angew. Chem. Int. Ed. 2022, 61, e202204108.

Table S2 The Pt content on the typical samples by ICP analysis.

Smaples	Pt / wt/%
Pt/Mn-TBAPy-SC	0.32
Pt/Mn-TBAPy-NT	0.33

For the photocatalytic water reduction, the amount of photocatalyts is 20 mg, the Pt weight percentages are measured and calculated by the sample weight. The H_2 evolution rates of both samples were normalized according to the Pt amounts (Fig. S12).

Table S3 Fitting parameters for the TA kinetics shown in Fig. 3a, Fig. 3b, and Fig. S16. The kinetics are fitted by a multi-exponential function.

MOFs	Wavelength / nm	τ_1 / ps (a_1)	τ_2 / ps (a_2)	τ_3 / ns (a_3)
Mn-TBAPy-SC	630	7.9 (15.9%)	1940 (73.6%)	> 10 (10.5%)
	730	7.9 (12.9%)	1940 (87.1%)	
Mn-TBAPy-NT	609	46.6 (14.7%)	1880 (34.8%)	> 10 (50.6%)
	690	6.7 (58.4%)	1880 (27.4%)	> 10 (14.2%)
Pt/Mn-TBAPy-SC	630	9.2 (35.5%)	3350 (64.5%)	/
Pt/Mn-TBAPy-NT	609	321.9 (24.9%)	3940 (75.1%)	/

The decay processes were fitted by the following multi-exponential function:

$$TA\,(t) = A_1 e^{-\frac{t}{\tau_1}} + A_2 e^{-\frac{t}{\tau_2}} + A_3 e^{-\frac{t}{\tau_3}} + \ldots + A_n e^{-\frac{t}{\tau_n}} \quad (2)$$

Table S4 Fitting parameters of combined fs and ns TA kinetics as shown in Fig. 3c and Fig. 3d.

MOFs	τ_1 / ps (a_1)	τ_2 / ns (a_2)	τ_3 / ns (a_3)	τ_4 / ms (a_4)	τ_{ave} / ns
Mn-TBAPy-SC	7.9, fixed (18.7%)	1.9, fixed (74.1%)	44.4 (7.1%)	/	4.6
Pt/Mn-TBAPy-SC	7.9, fixed (33.4%)	1.9, fixed (59.1%)	41.4 (7.5%)	/	4.2
Mn-TBAPy-NT	46.6,fixed (16.1%)	1.9, fixed (32.0%)	22.8 (44.7%)	3.4 (7.2%)	255.6
Pt/Mn-TBAPy-NT	/	0.15 (13.4%)	2.1 (69.2%)	0.05 (17.4%)	10.6

The whole TA kinetics of the internal charge-separated (ICS) state of Mn-TBAPy-SC and Pt/Mn-TBAPy-SC samples can be described by the following function:

$$TA\,(t) = A_1 e^{-\frac{t}{\tau_1}} + A_2 e^{-\frac{t}{\tau_2}} + A_3 e^{-\frac{t}{\tau_3}} \quad (3)$$

where τ_1 represents exciton-exciton annihilation time, τ_2 and τ_3 represent the decay lifetime of excitonic state and internal charge-separated (ICS) state that different from the excitonic state, respectively. We fixed the ultrafast component of τ_1 and a_1 obtained via the fitting of fs-TA kinetics (Table S3), and τ_2 and τ_3 as the free fitting parameters.

The TA kinetics of internal charge-separated (ICS) states were described by a four-exponential function because of the existence of a fast rising kinetics in Mn-TBAPy-NT and Pt/Mn-TBAPy-NT samples:

$$TA\,(t) = A_1 e^{-\frac{t}{\tau_1}} + A_2 e^{-\frac{t}{\tau_2}} + A_3 e^{-\frac{t}{\tau_3}} + A_4 e^{-\frac{t}{\tau_4}} \quad (4)$$

where τ_1 represents the excitonic-state-to-ICS transfer time in Mn-TBAPy-NS, τ_3 and τ_4 represent the decay lifetimes of the ICS states. When fitting the kinetics, τ_1 and τ_2 were fixed as constants according to the fitting results of fs-TA kinetics (Table S3), and τ_3, τ_4 were set as the free fitting parameters.

Table S5 Fitting parameters for the PL kinetics shown in Fig. 3e. The kinetics are fitted by a multiple-exponential function.

MOFs	A_1	τ_1 / ns	A_2	τ_2 / ns	Average time / ns
Mn-TBAPy-NT	0.28	0.86	0.60	17.88	12.45
Pt/Mn-TBAPy-NT	0.24	2.73	0.60	0.58	1.19
Mn-TBAPy-SC	0.42	0.51	0.48	2.81	1.69
Pt/Mn-TBAPy-SC	0.47	0.53	0.47	0.53	0.53

Table S6 The fitting parameters of photocatalyst electrodes.

Smaples	R_s /Ω	R_{ct} /Ω
Mn-TBAPy-SC	15	308240
Pt/Mn-TBAPy-SC	12	222600
Mn-TBAPy-NT	15	61000
Pt/Mn-TBAPy-NT	20	30010

Table S7 Hall measurement parameters of the photocatalysts.

Samples	Resistivity/ Ω cm^{-1}	Migration rate/ cm^2/V.S	Carrier concentration/cm^{-3}	Hall coefficient/ cm^3 C^{-1}
Mn-TBAPy-SC	3.13E-2	0.449	4.45E+18	-1.41E-4
Mn-TBAPy-NT	2.15E-2	0.489	8.03E+18	-1.23E-4

Table S8 Fitting parameters of Mn K-edge EXAFS curves for different samples.

Samples	Path	CN	R (Å)	σ^2 ($\times 10^{-3}$ Å^2)	ΔE_0 (eV)	R (%)
Mn-TBAPy-SC[a]	Mn-O	5.1±0.5	2.10±0.01	5.6±1.2	-3.45±0.89	0.4
Mn-TBAPy-NT[b]	Mn-O	4.9±0.4	2.14±0.01	7.4±1.5	-2.21±0.88	0.4
Mn foil[c]	Mn-Mn	12	2.67±0.01	5.9±1.7	6.82±1.69	1.5
MnO[d]	Mn-O	6	2.22±0.02	10.7±2.7	-1.79±2.25	1.2
	Mn-Mn	12	3.14±0.01	9.5±1.2	-4.65±1.30	
MnO$_2$[e]	Mn-O	6	1.89±0.02	2.4±1.0	-4.27±3.33	1.1

N, coordination number; R, distance between absorber and backscatter atoms; σ^2, Debye-Waller factor to account for both thermal and structural disorders; ΔE_0, inner potential correction; R factor (%) indicates the goodness of the fit. S_0^2 was fixed to 0.8 as determined from Mn foil fitting.
[a] Fitting range: $2.4 \leq k$ (/Å) ≤ 11.4 and $1.0 \leq R$ (/Å) ≤ 2.1.
[b] Fitting range: $2.3 \leq k$ (/Å) ≤ 10.4 and $1.0 \leq R$ (/Å) ≤ 2.2.
[c] Fitting range: $2.5 \leq k$ (/Å) ≤ 12.4 and $1.9 \leq R$ (/Å) ≤ 2.8.
[d] Fitting range: $2.5 \leq k$ (/Å) ≤ 12.8 and $1.0 \leq R$ (/Å) ≤ 3.1.
[e] Fitting range: $2.6 \leq k$ (/Å) ≤ 11.7 and $1.0 \leq R$ (/Å) ≤ 1.8.

References

1 Y. Xiao, X. Guo, T. Yang, J. Liu, X. Liu, Y. Xiao, L. Liu, T. Liu, S. Ye, J. Jiang, F. Zhang and C. Li, *Sci. China Chem.*, 2020, **63**, 1756-1760.
2 Q. Wang and K. Domen, *Chem. Rev.*, 2020, **120**, 919-985.